ELSEVIER

Biophysical Chemistry 95 (2002) 165–172

Biophysical Chemistry

www.elsevier.com/locate/bpc

Molecular characterization of a ligand-tethered parathyroid hormone receptor

Luca Monticelli[a,b], Stefano Mammi[b], Dale F. Mierke[a,*]

[a]*Department of Molecular Pharmacology, Division of Biology and Medicine, Box G-B4, Brown University, Providence, RI 02912, USA*

[b]*Department of Organic Chemistry, University of Padova, I-85747 Padova, Italy*

Received 12 December 2001; received in revised form 5 January 2002; accepted 8 January 2002

Abstract

It was recently shown that the covalent tethering of the N-terminus of parathyroid hormone (PTH) to the seventh helical bundle of the G-protein coupled PTH-receptor (PTH1R) leads to autoactivation [Shimizu et al., J. Biol. Chem. 275 (2000) 19456–19460]. Here, we have developed molecular models for the interaction of PTH(1–11) tethered to PTH1R and refined them with molecular dynamics simulations. The starting structure of the ligand/receptor complex is based on experimental data from a series of spectroscopic structural studies of PTH(1–34) and the extracellular domains of PTH1R and intermolecular contact points derived from photoaffinity labeling. The resulting PTH1R/[Arg^{11}]PTH(1–11) complex has the N-terminus of PTH interacting with residues of the third extracellular loop of PTH1R, as a possible mode for receptor activation. The hydrophobic residues leucine-5 and methionine-8, centrally located in the N-terminal α-helix of PTH(1–11), are located in deep, well-defined hydrophobic pockets in the central core of the seventh helical bundle, consistent with the requirement of these amino acids for autoactivation. We postulate that the improved signaling properties of [Arg^{11}]PTH(1–11) over wild type PTH(1–11) is due to a stable hydrogen bond between Arg^{11} and E444, at the beginning of TM7. The model provides atomic insight into currently available biochemical data as well as numerous putative ligand/receptor interactions, and thereby may further the rational design of reduced-size PTH agonists at the PTH1 receptor.

Keywords: Parathyroid hormone (PTH); PTH receptor; G-protein coupled receptors; Coupling of G-proteins to PTH receptor; Constitutively active receptors; Tethered-ligand

1. Introduction

Parathyroid hormone (PTH) is vital in the regulation of extracellular calcium homeostasis [1,2]. The receptor for PTH (PTH1R) is a member of the B family of G-protein coupled receptors, a class which includes receptors for secretin, calcitonin, glucagon and pituitary adenylate cyclase activating polypeptide. The receptor activates both G_s (associated with adenylyl cyclase/cyclic adenosine monophosphate/protein kinase A pathway) and G_q (inositol triphosphate/cytosolic calcium/protein kinase C) [3–8]. PTH1R is also activated

*Corresponding author. Tel.: +1-401-863-2139; fax: +1-401-863-1595.

E-mail address: dale_mierke@brown.edu (D.F. Mierke).

0301-4622/02/$ - see front matter
PII: S0301-4622(02)00005-4

by parathyroid hormone-related protein (PTHrP), a 141-residue protein, associated with skeletal development and the formation of cartilage [9,10]. The N-terminal 13 residues of PTH and PTHrP share 70% sequence homology. The report of PTH leading to increased bone density has suggested that the development of an agonist for PTH1R may provide a treatment for osteoporosis [11]. An understanding of the molecular mechanism by which the hormone is recognized and binds to its receptor should greatly facilitate these efforts.

By employing site-directed mutagenesis, receptor chimera and photoaffinity labeling, insight into the ligand/receptor complex has been obtained [12–17]. These data have clearly defined interactions between the seven helix bundle of the receptor and the N-terminus of the ligand. Similarly, interactions between the N-terminus of PTH1R and the C-terminus of the ligand have been shown to be a determinant for binding. Many of these data have been incorporated into a molecular model of the ligand/receptor complex [18]. The model was greatly enhanced by knowledge of the structural preferences of the extracellular domains of PTH1R as determined by high-resolution NMR in a lipid environment [19–21]. Despite these inroads, many questions regarding the ligand–receptor interactions, and certainly the mechanism of receptor activation, remain undefined. Too many degrees of freedom remain, particularly within the large N-terminus of the receptor, for which the structure is not known, and its role in facilitating the binding of PTH [22].

Recently, Gardella and co-workers have established a tethered ligand system for PTH1R which is constitutively active [23]. In this system, residues 1–181 of PTH1R are replaced with the N-terminus of PTH, PTH(1–9) or PTH(1–11), connected by a linker of four consecutive glycine residues. Additionally, in the PTH(1–11) tethered system, replacing Leu^{11} with Arg^{11} enhanced the autoactivation [23]. The tethered receptor lacks most of the extracellular N-terminus of PTH1R [the first transmembrane (TM) helix has been shown to begin at residue 190 [19]]. Most importantly for characterization of the ligand/receptor complex, the tethered ligand system greatly reduces the possible orientations of the ligand while bound to the receptor. Utilizing ligand/receptor contact points between PTH and PTH1R from photoaffinity labeling experiments [15] and the structural features of PTH [24], the topological orientation of the tethered-ligand within the receptor is further defined.

Here, we present results from our examination of the PTH1R/[Arg^{11}]PTH(1–11) tethered system by extensive computer simulations, providing molecular insight into ligand/receptor interactions. We show that our findings are in accordance with results from site-directed mutagenesis, receptor chimera and photoaffinity labeling carried out on the wild-type PTH-PTH1R system. Such details should facilitate ongoing efforts to increase the binding affinity of exogenous N-terminal fragments of PTH [25,26] as a novel route for the treatment of osteoporosis [11,27].

2. Methods

The model of the PTH1R/[Arg^{11}]PTH(1–11) tethered receptor was generated using previously published methods [18,28]; new mutational data were incorporated into the model, as were the conformational features of three of the loops connecting the transmembrane (TM) helices, recently determined by NMR spectroscopy in our laboratory [19,29]. The arrangement of the TM helices was updated based on the X-ray structure of bovine rhodopsin [30].

The modeling of the tethered ligand (positions 1–11 of the mutant receptor) utilized the structure of PTH(1–34), previously determined in a micellar-lipid environment in our laboratory [24]. The backbone dihedral angles of the connecting flexible region 12–15, constituted by four consecutive glycines, were rotated manually until the helix of the ligand was above the putative binding site, at the extracellular surface, above the central core of the TM helical bundle. The conformation of the short N-terminal region (segments 182–198) was assumed to be similar to that determined by NMR in a lipid environment for the fragment 168–198 [19]: the region from 182 to 189 was an α-helix lying on the surface of the membrane and the α-helix forming the extracellular end of TM1 was composed of residues 190–198. The resulting

receptor was energy-minimized and subjected to a short MD run (in vacuo) using the DISCOVER program (Molecular Simulations Inc.) in order to remove initial strain. During this stage, the TM helices were restrained to their initial positions using template forcing.

Only one of the contact points generated from the photo-affinity labeling studies involves residues in segments 1–11 of PTH (a covalent attachment between position 1 of the hormone and position 425 of the receptor [15]). A distance restraint between these residues of 0.7 nm was used in the subsequent stages of the refinement. The loose distance restraint (0.7 nm) is used, although proton extraction of the photo-excited species is limited to 0.31 nm [31], to compensate for the replacement of the natural amino acid (Ser^1 replaced by the benzoyl phenylalanine used for photoaffinity labeling).

The receptor was then soaked in a three-layer (water/decane/water) simulation cell for further refinement by MD simulations. The TM helices were embedded in the decane layer while the extra- and intracellular regions were placed in water phases. The membrane environment was mimicked by a layer of approximately 40 Å of decane molecules [32], with approximately 25 Å of water above and below, consisting of approximately 900 decane and 15 000 water molecules. The solvent system sacrifices the charged nature of the lipid/water interface for computational simplicity while maintaining the overall biphasic, hydrophobic/hydrophilic character, as well as the molecular motions of the long acyl-chains found in membranes. The CH_2 and CH_3 groups of decane were treated as united atoms, the Ryckaert–Bellemans potentials were applied, and a minimum distance of 2.3 Å between water and decane molecules was allowed [32]. All solvated simulations and their analysis were carried out using the GROMACS package, version 2.0 [33].

The refinement consisted of three stages. In the first stage, the solvent was allowed to equilibrate during a 50-ps MD run at 300 K, while the heavy atoms of the protein were constrained in their initial positions, with a force constant of 1000 kJ mol^{-1} nm^{-2}. In the second stage, 300 ps of restrained MD at 300 K were performed using the distance restraint between Ser^1 and M425. During the final stage, the distance restraint was removed and the system was allowed to evolve freely for 2 ns of MD at 300 K. The RMSD of the atomic coordinates and of interatomic distances for the backbone atoms was monitored during the simulation. Representative structures were obtained for each MD run by energy minimization of the average coordinates over the last 500 ps of simulation.

All simulations were carried out using periodic boundary conditions and neighbor lists for the calculation of non-bonded interactions, updated every 10 steps. Only non-bonded interactions within 1.0 nm were included, both for the calculation of the Lennard–Jones and the electrostatic potential. Temperature and pressure bath coupling were applied [34,35], with time constants of 0.02 and 1 ps, respectively. All calculations were performed on an SGI Origin 2000 computer and on a 6-PC cluster with Linux operating system.

3. Results and discussion

The starting point for the simulations of the tethered-ligand receptor system include the topological orientation of the TM helices based on the X-ray structure of rhodopsin [30], ligand/receptor contact points derived from photo-affinity labeling experiments [15], and the structural preferences of the ligand and the extracellular domains of the receptor as determined by NMR studies [19,24]. The general applicability of the structural features of the TM helices of rhodopsin as a template has been addressed in some detail in the literature [36–42]. We have previously shown that the rhodopsin model for the PTH1 receptor places R233 (TM2) and Q451 (TM7) facing each other in the central TM core of the receptor [18]. Experimentally, Gardella and co-workers have shown that an interaction between these residues is important for binding of PTH and signaling [43]. In our model, both R233 and Q451 are located in the middle of their respective TM helices, projecting towards each other with an average distance of 0.25 nm between the side chains during the MD simulations. Additional evidence for rhodopsin as a

template was provided by the incorporation of zinc-binding pockets into the PTH1 receptor [44].

The structural features of PTH have been extensively examined over the years (see recent review [27]). All of these studies agree that the N-terminus of the ligand has a strong propensity to form an α-helix. Our own studies of human PTH(1–34) in the presence of lipids [24] showed a well-defined α-helix between the residues Ser^{3}–Asn^{10}. Structural studies of reduced-size PTH analogs, PTH(1–14), likewise display a large percentage of α-helix based on CD measurements [26]. Therefore, the starting structure of the tethered receptor contained an α-helix for residues 3–10 of the ligand. Likewise, from our NMR-based structural studies of the proximal N-terminus of the receptor [19], an α-helix, lying on the surface of the membrane environment, was incorporated into the starting structure for residues 182–189 of the receptor. The TM1 helix was assumed to begin just following this helix at residue 190, based on the experimental findings of our previous study [19].

The ligand was placed within the receptor to account for the photo-affinity derived contact points between M425 (TM6) and residues 1 and 2 of the ligand [15,45]. These interactions between the N-terminus of the ligand and the extracellular face of TM6 require the ligand to extend across the seventh helical bundle of the receptor (Fig. 1). Utilizing this starting structure, extensive MD simulations were carried out using a water/decane/water simulation cell [19,46]. No major conformational changes take place during the MD simulation (an average RMSD over the simulation trajectory with the starting structure is 0.13 nm for the heavy backbone atoms). Below, the results from the simulations and the agreement with experimental data are detailed starting with the N-terminus of the ligand.

3.1. Residue Ala^{1}

In the model, the N-terminal residue of PTH is located on the top of TM6, very close to EC3. The positively charged, amino group of Ala^{1} is hydrogen-bonded to the backbone carbonyl groups of residues M425, A426 and T427 found in the final helical-turn of TM6. The interaction between the positive charge and the macro-dipole of the helix is very favorable (positive charges are often observed at the C-terminal ends of α-helices in protein structures). The amino group of PTH(1–34) was found to form similar interactions in the previously published model of PTH1R/PTH(1–34) [18]. Importantly, removal of the NH_3^+ leads to a great reduction of the activity of PTH(1–34) [47]. Therefore, we conclude that this interaction is determinant for receptor activation in both the wild type and ligand-tethered receptors.

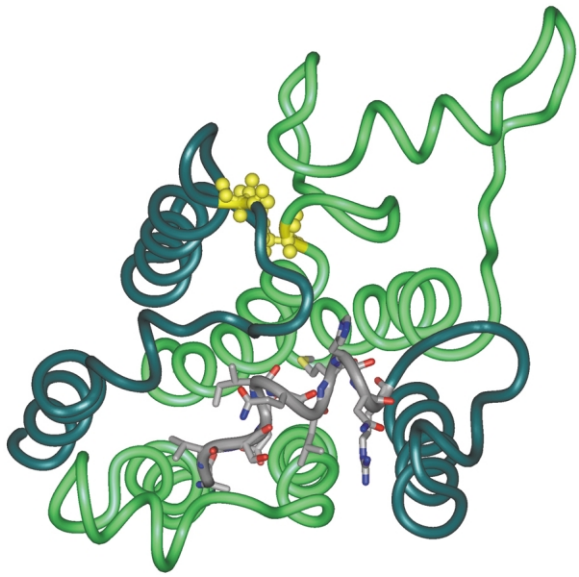

Fig. 1. Extracellular view of the PTH1R/[Arg^{11}]PTH(1–11) tethered receptor system. TM1 (lower right) and TM4-EC2-TM5 (upper left) are displayed in dark green. The [Arg^{11}]PTH(1–11) ligand is shown in gray with the side chains depicted as sticks. The disulfide bond between EC2 and TM3 is illustrated in yellow.

In the model, M425, which is found to crosslink to position 1 of PTH(1–34) [15], is located on the extracellular end of TM6 projecting towards the membrane, away from the core of the TM-helix bundle and at an average distance of approximately 0.65 nm away from Ser^{1} of PTH. We postulate that the longer, much more hydrophobic benzoyl phenylalanine utilized in photoaffinity labeling experiments projects further out, between TM5 and TM6, into the membrane environment,

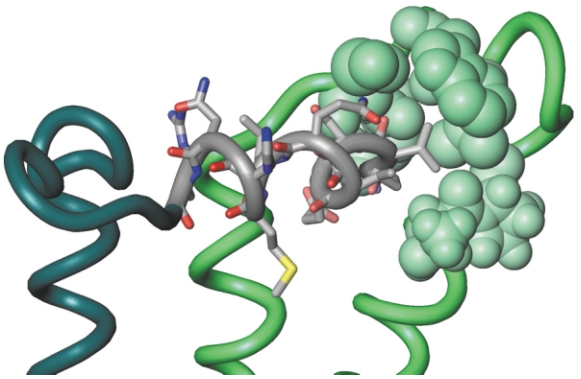

Fig. 2. Depiction of the hydrophobic binding pocket of Val^2 of [Arg^{11}]PTH(1–11). The residues contributing to the pocket (see text) are depicted as CPK spheres.

and therefore, comes quite close to M425 (closer than the upper limit of 0.31 nm for proton extraction by the photo-excited species).

3.2. Residue Val^2

In the model, Val^2 is located in a hydrophobic pocket, as shown in Fig. 2, formed by four residues in EC3: L436, W437, Q440 and M441. The binding pocket is a direct result of the presence of an α-helix in the third extracellular loop of PTH1R as determined by NMR in our laboratory and of the small size of the loop (approx. 12 residues). Previous mutations have probed this binding pocket. According to Lee et al., substitution of W437 (with A, L or E) or Q440 (with A or L) in PTH1R leads to a loss in PTH(1–34) binding, an effect much reduced with PTH(3-34) [13]. The results from the simulations provide molecular insight into these mutations. W437 and Q440 are located in the short α-helical segment of EC3. In the absence of a ligand, we hypothesize that these residues, certainly the tryptophan, are projecting towards the membrane. Upon ligand binding, we observe that W437 and Q440 contribute to a hydrophobic pocket for Val^2. This change is brought about by a slight rotation of the central helix of EC3 and rotamer transition of the χ_1 side chain dihedral angle of W437. Replacing these residues with smaller or more polar amino acid would disrupt the favorable interaction with Val^2 of the ligand. With truncation of the N-terminus and the removal of Val^2, i.e. PTH(3–34), this would not be an issue. From our model, substitution of Q440 with a positively charged arginine would lead to a favorable Coulombic interaction with Glu^4 of the N-terminus of PTH, while maintaining the hydrophobic pocket for Val^2 of the ligand.

Within the tethered-ligand receptor system, Val^2 is important for autoactivation; replacement of Val^2 with Ala^2, leads to a dramatic decrease in cAMP production [23]. Based on our model, we propose that the smaller alanine does not fill the hydrophobic pocket, disrupting the interaction of the N-terminus of the ligand with the EC3 of the receptor, a step we hypothesize to be determinant for receptor activation.

3.3. Residue Ser^3

During the simulations carried out here, Ser^3 is found projecting away from the receptor, exposed to the aqueous solution. The residue is in close proximity to the central helix of EC3, which we predict places limits on the size of residue side chain at this position. An alanine scan of the PTH1R/PTH(1–11) tethered system indicates only a minor role for Ser^3 with respect to autoactivation [23]. In standard activity assays with PTH(1–34), the Ser^3/Ala^3 substitution produces only small changes in the EC_{50} values [48]. For the PTH(1–14) system, only serine, glycine and alanine preserved high affinity of the ligand for PTH1R [49].

3.4. Residue Glu^4

During the simulations, Glu^4 is found projecting towards EC3 and the extracellular end of TM7, in a binding pocket formed by the aromatic residues, Y443 and F447. During the simulations, the negatively charged side chain is found to form a hydrogen bond with Q440. Replacement of Glu^4 with Ala^4 leads to a significant drop in the autoactivation of the PTH(1–11) tethered ligand [23]. Similarly, Glu^4 is found to be imperative in PTH(1–14) in standard activity assays [49]. As mentioned above, the Q440 has been shown to

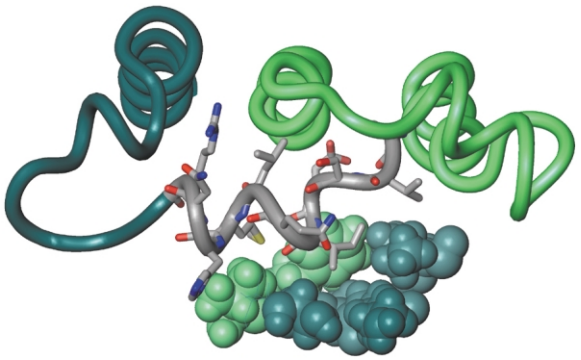

Fig. 3. Depiction of the hydrophobic binding pocket of Ile^5 of [Arg^{11}]PTH(1–11). The residues contributing to the pocket (see text) are depicted as CPK spheres.

play an important role in the activation of PTH1R, replacement with Leu or Ala producing a precipitous drop in ligand binding.

3.5. Residue Ile^5

In the model, the side chain of Ile^5 is accommodated by a hydrophobic pocket made up of the extracellular ends of TM3 (F287, V283), TM7 (F447, F450) and EC2 (I362), which forms the bottom of the pocket, as illustrated in Fig. 3. The binding cavity extends deep into TM3, TM4, TM5 and TM6, in a very similar fashion to that previously observed in the PTH/PTH1R model [18].

The results from the alanine scan confirm the importance of the interactions involving this residue for autoactivation: substitution of Ile^5 with an alanine markedly reduces cAMP production. Previous functional studies on PTH(1–14) [25,49], PTH(1–34) and PTHrP(1–36) [48,50] have also illustrated a vital role for the residue at this position.

3.5.1. Residue Gln^6

The hydrophilic amino acid is projecting away from the receptor, exposed to water. Replacement with an alanine does not significantly alter autoactivation [23], which is in contrast to the results of mutation of this residue in wild-type receptor activation assays with PTH(1–14) and PTH(1–34).

3.6. Residue Leu^7

This residue is projecting towards the extracellular end of TM7. A hydrophobic pocket is formed at the beginning of TM7 by the aromatic residues H442, Y443 and F447. Such a binding pocket of aromatic residues is consistent with the findings that the replacement of Leu^7 with Phe^7 in PTH(1–14) increases cAMP production in wild-type receptor-bases assays [49]. Within the tethered PTH(1–11) system, replacement of Leu^7 with an alanine leads to a 50% reduction in cAMP production [23].

3.7. Binding pocket for residue Met^8

The side chain of Met^8 is found on the same face of the N-terminal helix as Ile^5, in a deep hydrophobic pocket made up of the extracellular termini of TM2, TM3 and TM7, involving residues K238, F287, V283 and F447. The finding of a hydrophobic pocket is consistent with the observation that, in PTH(1–34), oxidation of Met^8 results in a decrease in the biological response [51], and that replacement of this Met with norleucine is well tolerated, producing no loss of binding affinity [52]. In the tethered ligand receptor system, Met^8 is strictly required for autoactivation [23].

3.8. His^9, Asn^{10}

During the MD simulations both of these residues interact with the receptor only minimally. In the tethered PTH(1–11) system examined here, replacement of His^9 with an alanine, leads to only a slight reduction of the production of cAMP levels, which may be indicative of this position exposed to the aqueous environment and therefore favoring histidine. These findings are in accordance with the mutational results observed for Asn^{10} of PTH(1–14), which indicate that most hydrophilic amino acids are well tolerated at this position [49].

3.9. Interactions of Arg^{11}

The model also provides an explanation for the increased basal cAMP levels upon the substitution of Leu^{11} (naturally found in PTH) with Arg^{11}. The

results of the MD simulations show that Arg^{11} is between Y191 and E444 located at the extracellular ends of TM1 and TM7, respectively. A hydrogen bond between Arg^{11} and E444 is prominent during the MD simulations (observed for 86% of the simulation with an average distance of 0.26 nm). Given the high intrinsic flexibility of the N-terminus of the receptor (due to the four consecutive glycines in position 12–15), this hydrogen bond may be critical for stabilizing the activated conformation of the molecule. In fact, this interaction provides an anchoring point for the tethered ligand, keeping the ligand centrally located in the seventh helical bundle. This anchoring point is not necessary for the binding of PTH(1–34) to the wild type receptor, in which a large number of interactions between the C-terminus of the ligand and N-terminus of the receptor are present. In the previously published model of the PTH1R/PTH(1–34) complex [18], the side chain of Leu^{11} of the ligand is found in almost the same position, between residues E444, I190 and Y191. It should be noted that PTHrP contains Lys^{11}, indicating that this hydrogen bond may be active in the binding of this related hormone to PTH1R.

3.10. Interactions of F184, L187 of PTH1R

In the resulting structures from the simulations, these two hydrophobic residues, just proximal to the beginning of TM1, are projecting into the decane, serving to anchor the polyGly-ligand close to the membrane surface (Fig. 4). During the NMR-study of PTH1R(168–198), the intensity of the signals of both F184 and L187 were greatly reduced upon the addition of a nitroxide-radical to the lipid micelles [19], providing experimental evidence for the interaction with the alkyl-chains of the lipids. Indeed, Gardella and co-workers have found that both of these positions can be replaced with hydrophobic amino acids (e.g. Ile, Met, Leu) without loss of biological function, while hydrophilic amino acids (e.g. Asp, Glu, Lys, Arg) are not tolerated [53]. These experimental findings are in full accordance with the structures developed here.

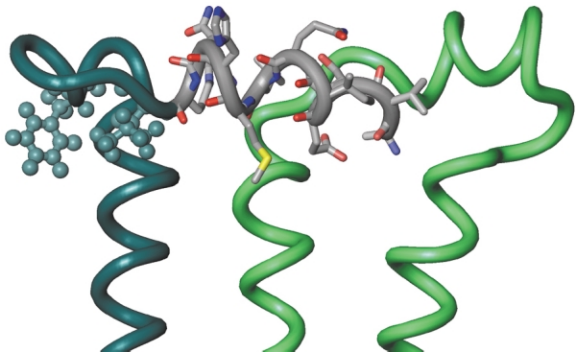

Fig. 4. Side view of the ligand tethered to TM1. The ligand is parallel to the α-helix in the center of EC3, which lies along the membrane surface. Both F184 and L187 are shown as ball-and-stick models, projecting towards the hydrophobic environment of the membrane, serving to anchor the ligand in the correct orientation to bind to the receptor.

4. Conclusions

The tethering of the PTH to its G-protein coupled receptor has provided a unique vehicle to examine the determinants required for receptor activation. The deletion of a majority of the large N-terminus (residues 1–181), leaving only the TM helical bundle, greatly simplifies our efforts to structurally probe the ligand–receptor interactions. Likewise, employing only the N-terminus of PTH (residues 1–11), which forms a stable, well-determined α-helix [24], and removes points of flexibility or regions which are structurally undefined. These simplifications of the ligand/receptor system coupled with the experimentally determined conformations of the extracellular domains of PTH1R [19,21] and photoaffinity labeling data provide for a very well determined starting point for MD simulations. The resulting structures from the simulations suggest a number of ligand/receptor interactions. Some of the sites of the receptor identified here have been previously examined by site-directed mutagenesis and are shown to play a role in receptor function. Our results suggest how and where these receptor residues interact with the ligand. Based on these results, we aim to design more conformational constrained reduced size analogs of PTH, an important target for the treatment of osteoporosis [11].

References

[1] M. Rosenblatt, Pathobiol. Annu. 11 (1981) 53–86.
[2] J.T. Potts, H.M. Kronenberg, M. Rosenblatt, Adv. Protein Chem. 35 (1982) 323–396.
[3] A.B. Abou-Samra, S. Uneno, H. Jueppner, et al., Endocrinology 125 (1989) 2215–2217.
[4] A. Iida-Klein, V. Varlotta, T.J. Hahn, J. Bone Miner. Res. 4 (1989) 767–774.
[5] R. Civitelli, T.J. Martin, A. Fausto, S.L. Gunsten, K.A. Hruska, L.V. Avioli, Endocrinology 125 (1989) 1204–1210.
[6] H. Jüppner, A.B. Abou-Samra, M. Freeman, et al., Science 254 (1991) 1024–1026.
[7] A.B. Abou-Samra, H. Jüppner, A. Khalifa, et al., Endocrinology 132 (1993) 801–805.
[8] M. Pines, S. Fukayama, K. Costas, et al., Bone 18 (1996) 381–389.
[9] J.J. Wysolmerski, A.F. Stewart, Annu. Rev. Physiol. 60 (1998) 431–460.
[10] W.M. Philbrick, J.J. Wysolmerski, S. Galbraith, et al., Physiol. Rev. 76 (1996) 127–173.
[11] P. Morley, J.F. Whitfield, G.E. Willick, Curr. Pharm. Des. 7 (2001) 671–687.
[12] C. Lee, T.J. Gardella, A.B. Abou-Samra, et al., Endocrinology 135 (1994) 1488–1495.
[13] C. Lee, M.D. Luck, H. Juppner, J.T. Potts, H.M. Kronenberg, T.J. Gardella, Mol. Endocrinol. 9 (1995) 1269–1278.
[14] M. Mannstadt, M.D. Luck, T.J. Gardella, H. Juppner, J. Biol. Chem. 273 (1998) 16890–16896.
[15] A. Bisello, A.E. Adams, D.F. Mierke, et al., J. Biol. Chem. 273 (1998) 22498–22505.
[16] Z. Greenberg, A. Bisello, D.F. Mierke, M. Rosenblatt, M. Chorev, Biochemistry 39 (2000) 8142–8152.
[17] R.C. Gensure, T.J. Gardella, H. Juppner, J. Biol. Chem. 276 (2001) 28650–28658.
[18] C. Roelz, M. Pellegrini, D.F. Mierke, Biochemistry 38 (1999) 6397–6405.
[19] M. Pellegrini, A. Bisello, M. Rosenblatt, M. Chorev, D.F. Mierke, Biochemistry 37 (1998) 12737–12743.
[20] M. Pellegrini, D.F. Mierke, J. Peptide Sci. 51 (1999) 208–220.
[21] A. Piserchio, A. Bisello, M. Rosenblatt, M. Chorev, D.F. Mierke, Biochemistry 39 (2000) 8153–8160.
[22] U. Grauschopf, H. Lilie, K. Honold, et al., Biochemistry 39 (2000) 8878–8887.
[23] M. Shimizu, P.H. Carter, T.J. Gardella, J. Biol. Chem. 275 (2000) 19456–19460.
[24] M. Pellegrini, M. Royo, M. Rosenblatt, M. Chorev, D.F. Mierke, J. Biol. Chem. 273 (1998) 10420–10427.
[25] M.D. Luck, P.H. Carter, T.J. Gardella, Mol. Endocrinol. 13 (1999) 670–680.
[26] M. Shimizu, P.H. Carter, A. Khatri, J.T. Potts, T.J. Gardella, Endocrinology 142 (2001) 3068–3074.
[27] D. Mierke, M. Pellegrini, Curr. Pharm. Des. 5 (1999) 21–36.
[28] C. Roelz, D.F. Mierke, Biophys. Chem. 89 (2001) 119–128.
[29] A. Piserchio, G. Prado, L. Taylor, P. Polgar, D.F. Mierke, Mol. Pharm. (2001) submitted.
[30] K. Palczewski, T. Kumasaka, T. Hori, et al., Science 289 (2000) 739–745.
[31] M.A. Winnik, Chem. Rev. 81 (1981) 491–534.
[32] A.R. van Buuren, S. Marrink, H.J.C. Berendsen, J. Phys. Chem. 97 (1993) 9206–9216.
[33] H.J.C. Berendsen, D. van der Spoel, R. van Buuren, Comp. Phys. Comm. 95 (1995) 43–56.
[34] H.J.C. Berendsen, J.P.M. Postma, A. DiNola, J.R. Haak, J. Chem. Phys. 81 (1984) 3684–3690.
[35] W.F. van Gunsteren, H.J.C. Berendsen, Angew. Chemie. Int. Ed. Engl. 29 (1990) 992–1023.
[36] J.M. Baldwin, EMBO J. 12 (1993) 1693–1703.
[37] H.R. Bourne, Curr. Opin. Cell Biol. 9 (1997) 134–142.
[38] D. Donnelly, FEBS Lett. 409 (1997) 431–436.
[39] J.M. Baldwin, G.F. Schertler, V.M. Unger, J. Mol. Biol. 272 (1997) 144–164.
[40] C. Czaplewski, R. Kazmierkiewicz, J. Ciarkowski, J. Comput. Aided Mol. Des. 12 (1998) 275–287.
[41] M. Beck, T.P. Sakmar, F. Siebert, Biochemistry 37 (1998) 7630–7639.
[42] K.K. Jensen, L. Martini, T.W. Schwartz, Biochemistry 40 (2001) 938–945.
[43] T.J. Gardella, M.D. Luck, M.H. Fan, C. Lee, J. Biol. Chem. 271 (1996) 12820–12825.
[44] S.P. Sheikh, J.P. Vilardarga, T.J. Baranski, et al., J. Biol. Chem. 274 (1999) 17033–17041.
[45] V. Behar, A. Bisello, G. Bitan, M. Rosenblatt, M. Chorev, J. Biol. Chem. 275 (2000) 9–17.
[46] G.N. Prado, D.F. Mierke, M. Pellegrini, L. Taylor, P. Polgar, J. Biol. Chem. 273 (1998) 33548–33555.
[47] H. Takasu, T.J. Gardella, M.D. Luck, J.T. Potts, F.R. Bringhurst, Biochemistry 38 (1999) 13453–13460.
[48] M. Chorev, M. Rosenblatt, in: J.P. Bilezikian, M.A. Levine, R. Marcus (Eds.), The Parathyroids, Raven Press, New York, 1994, pp. 139–156.
[49] M. Shimizu, J.T. Potts, T.J. Gardella, J. Biol. Chem. 275 (2000) 21836–21843.
[50] J.T. Potts, T.J. Gardella, H. Jüppner, H.M. Kronenberg, J. Endocrinol. 154 (1996) S15–S21.
[51] A.L. Frelinger, 3rd, J.E. Zull, J. Biol. Chem. 259 (1984) 5507–5513.
[52] M. Rosenblatt, D. Goltzman, H.T. Keutmann, G.W. Tregear, J.T. Potts, J. Biol. Chem. 251 (1976) 159–164.
[53] P.H. Carter, M. Shimizu, M.D. Luck, T.J. Gardella, J. Biol. Chem. 274 (1999) 31955–31960.